



저작자표시-비영리-변경금지 2.0 대한민국

이용자는 아래의 조건을 따르는 경우에 한하여 자유롭게

- 이 저작물을 복제, 배포, 전송, 전시, 공연 및 방송할 수 있습니다.

다음과 같은 조건을 따라야 합니다:



저작자표시. 귀하는 원저작자를 표시하여야 합니다.



비영리. 귀하는 이 저작물을 영리 목적으로 이용할 수 없습니다.



변경금지. 귀하는 이 저작물을 개작, 변형 또는 가공할 수 없습니다.

- 귀하는, 이 저작물의 재이용이나 배포의 경우, 이 저작물에 적용된 이용허락조건을 명확하게 나타내어야 합니다.
- 저작권자로부터 별도의 허가를 받으면 이러한 조건들은 적용되지 않습니다.

저작권법에 따른 이용자의 권리는 위의 내용에 의하여 영향을 받지 않습니다.

이것은 [이용허락규약\(Legal Code\)](#)을 이해하기 쉽게 요약한 것입니다.

[Disclaimer](#)

Differentiation between focal  
malignant-replacing lesions and benign  
red marrow deposition of the spine with  
T2\*-corrected fat-signal fraction map  
using a three-echo volume interpolated  
breath-hold gradient echo Dixon  
sequence



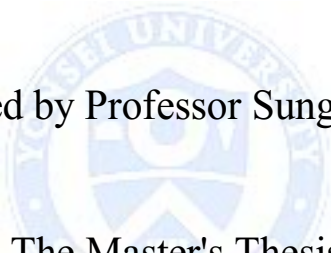
Yong Pyo Kim

Department of Medicine

The Graduate School, Yonsei University

Differentiation between focal  
malignant-replacing lesions and benign  
red marrow deposition of the spine with  
T2\*-corrected fat-signal fraction map  
using a three-echo volume interpolated  
breath-hold gradient echo Dixon  
sequence

Directed by Professor Sungjun Kim



The Master's Thesis  
submitted to the Department of Medicine,  
the Graduate School of Yonsei University  
in partial fulfillment of the requirements for the degree  
of Master of Medical Science

Yong Pyo Kim

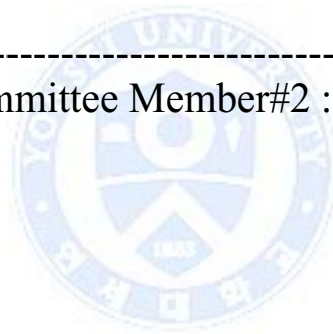
June 2015

This certifies that the Master's Thesis of  
Yong Pyo Kim is approved.

-----  
Thesis Supervisor : Sungjun Kim

-----  
Thesis Committee Member#1 : Choon-Sik Yoon

-----  
Thesis Committee Member#2 : Sunguk Kuh



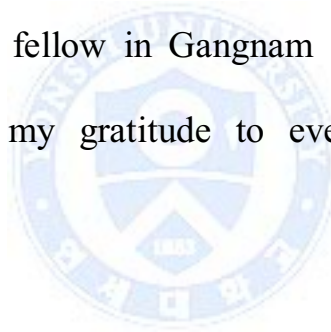
The Graduate School  
Yonsei University

June 2015

## ACKNOWLEDGEMENTS

I would like to thank to professor Sungjun Kim, Department of Radiology, Gangnam Severance hospital for the invaluable guidance and enthusiastic support. I am also very grateful to professor Choon-sik Yoon and professor Sunguk Kuh, thesis committee members for sincere advice.

As a radiology fellow in Gangnam Severance hospital, I wish to express my gratitude to every professor in the department.



## <TABLE OF CONTENTS>

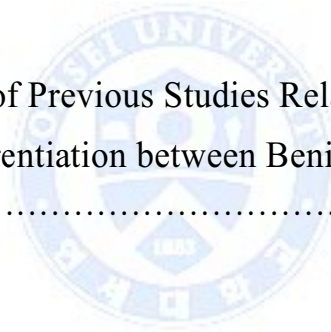
ABSTRACT .....	1
I. INTRODUCTION .....	3
II. MATERIALS AND METHODS .....	5
1. Patients .....	5
2. MR Imaging Protocol .....	7
3. Image Analysis .....	9
4. Statistical Analysis .....	13
III. RESULTS .....	14
IV. DISCUSSION .....	23
V. CONCLUSION .....	30
REFERENCES .....	31
ABSTRACT(IN KOREAN) .....	36
PUBLICATION LIST .....	38

## LIST OF FIGURES

Figure 1. Region of interest (ROI) placement and parameter measurement .....	11
Figure 2. An example of a false-negative result (erroneously defined as benign) of FF illustrated from MR images and a computed tomography (CT) image obtained from a 54-year-old man .....	18
Figure 3. An example of a false-positive result (erroneously defined as malignant) of LDR illustrated from MR images obtained from a 46-year-old woman .....	20
Figure 4. An example of a false-positive result (erroneously defined as malignant) of CER illustrated from MR images obtained from a 66-year-old woman .....	21
Figure 5. An example of a false-negative result (erroneously defined as benign) of CER illustrated from MR images obtained from a 42-year-old man .....	22

## LIST OF TABLES

Table 1. Summary of Analyzed MR Imaging Parameters .....	8
Table 2. Comparison of Median Values for the Parameters between Malignant-replacing Lesion and Benign Red Marrow Deposition Groups .....	16
Table 3. Diagnostic Performance of Each Parameter Determined Through Receiver Operating Characteristic Curve Analysis ..	17
Table 4. Summary of Previous Studies Related to Chemical-shift Imaging for Differentiation between Benign and Malignant Lesions .....	25



ABSTRACT

**Differentiation between focal malignant-replacing lesions and benign red marrow deposition of the spine with T2\*-corrected fat-signal fraction map using a three-echo volume interpolated breath-hold gradient echo Dixon sequence**

Yong Pyo Kim

*Department of Medicine  
The Graduate School, Yonsei University*

(Directed by Professor Sungjun Kim)

**Objective:**

To assess the feasibility of T2\*-corrected fat-signal fraction (FF) map by using the three-echo volume interpolated breath-hold gradient echo (VIBE) Dixon sequence to differentiate between malignant marrow-replacing lesions and benign red marrow deposition of vertebrae.

**Materials and Methods:**

We assessed 32 lesions from 32 patients who underwent magnetic resonance imaging after being referred for assessment of a known or possible vertebral marrow abnormality. The lesions were divided into 21 malignant marrow-replacing lesions and 11 benign red marrow depositions. Three sequences for the parameter measurements were obtained by using a 1.5-T MR imaging scanner as follows: three-echo VIBE Dixon sequence for FF;

conventional T1-weighted imaging for the lesion-disc ratio (LDR); pre- and post-gadolinium enhanced fat-suppressed T1WI for the contrast-enhancement ratio (CER). A region of interest was drawn for each lesion for parameter measurements. The areas under the curve (AUC) of the parameters and their sensitivities and specificities at the most ideal cutoff values from receiver operating characteristic curve analysis were obtained. AUC, sensitivity, and specificity were respectively compared between FF and CER.

**Results:**

The AUCs of FF, LDR, CER were 0.96, 0.80, and 0.72, respectively. In the comparison of diagnostic performance between FF and CER, FF showed a significantly larger AUC compared to CER ( $p = 0.030$ ), although the difference of sensitivity ( $p = 0.157$ ) and specificity ( $p = 0.157$ ) were not significant.

**Conclusion:**

Fat-signal fraction measurement using T2\*-corrected three-echo VIBE DIXON sequence is feasible and shows more accurate diagnostic performance than CER in distinguishing benign red marrow deposition from malignant bone marrow-replacing lesions.

---

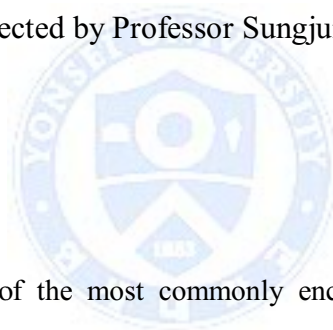
Key words : Magnetic resonance imaging; Spine; Fat signal fraction; Bone marrow.

**Differentiation between focal malignant-replacing lesions and benign red marrow deposition of the spine with T2\*-corrected fat-signal fraction map using a three-echo volume interpolated breath-hold gradient echo Dixon sequence**

Yong Pyo Kim

*Department of Medicine  
The Graduate School, Yonsei University*

(Directed by Professor Sungjun Kim)



**I. INTRODUCTION**

For physicians, one of the most commonly encountered scenarios during interpretation of conventional magnetic resonance (MR) imaging of the spine is differentiating neoplastic marrow infiltration from red marrow deposition.<sup>1</sup> Several methods can be used for this differentiation, such as diffusion-weighted imaging, chemical-shift imaging, dynamic contrast-enhanced imaging, MR spectroscopy.<sup>2,3</sup> We focused on chemical-shift imaging in this study.

Normal marrow is an intermixture of hematopoietically active (red) marrow and inactive (yellow) marrow supported by varying proportions of structural trabecular bone. Red and yellow marrow possess a substantial fat component.<sup>2-5</sup>

Hence, benign red marrow deposition generally shows higher signal intensity (SI) on T1-weighted images (T1WI) compared to sound muscle and the intervertebral disc.<sup>2,3</sup> On the other hand, the SIs of pathologic bone marrow lesions are generally similar to or lower than those of the muscle and disc, because the fat-containing bone marrow of the spine is replaced by tumor cells.<sup>5-7</sup> However, benign hypercellular red marrow may also show an unexpectedly low SI on T1-weighted imaging, similar to pathologic bone marrow lesions.<sup>3</sup> Many studies have tested in- and opposed-phase imaging for marrow lesion differentiation based on the expectation that the presence of fat in red marrow can cause the SI to drop on opposed-phase imaging.<sup>1,5,6,8,9</sup> We thought that lesions without fat, which can be seen in marrow replacing conditions, can theoretically show no or less signal drop in the opposed phase.

Hence, we commenced this study with the expectation that measurement of the fat-signal fraction (FF), considering T2\* decay bias correction,<sup>10,11</sup> could be feasible and may be more reasonable than indirect measurement of fat within a lesion with opposed-phase imaging. To the best of our knowledge, the utility of FF quantification to differentiate between malignant and benign marrow lesions has not been addressed.

Hence, the purpose of this study was to evaluate the feasibility of T2\*-corrected FF quantification by using three-echo gradient echo imaging with T2\* correction and Dixon water/fat separation to differentiate malignant marrow-replacing lesions from benign red marrow deposition of vertebrae.

## II. MATERIALS AND METHODS

### 1. Patients

The institutional review board reviewed our study and issued a waiver. All patients signed informed consent as part of their research hospital visits. From March 2012 to February 2013, 46 consecutive patients who were referred for MR imaging to evaluate a suspected spinal malignancy ( $n = 32$ ) or presented with an incidentally found marrow signal abnormality (defined as low or similar signal intensity to non-degenerated intervertebral disc on T1-weighted imaging [T1WI]) during MR imaging performed to assess the etiology of back or neck pain ( $n = 14$ ). These patients underwent an MR protocol including a FF mapping sequence, as described below. Patients who received radiotherapy on the marrow lesions ( $n = 5$ ) or systemic chemotherapy ( $n = 8$ ) prior to MR imaging were excluded because these treatments are known to cause unpredictable signal alterations that might affect FF.<sup>6</sup> One patient was excluded because of an uncorrectable calculation error; this error, which was found during image analysis, presumably occurred during image acquisition of the FF mapping sequence. Therefore, our study included 32 patients (17 women, 15 men; mean age,  $59.9 \pm 14.2$  [36–94] years) who underwent MR examination for naïve marrow lesions.

The subjects were divided into two groups based on the pathologic examination result or on the clinical and diagnostic imaging results, which were interpreted by two experienced musculoskeletal radiologists with 23 and 11

years of experience in spine imaging interpretation, respectively.

Group 1 consisted of 21 subjects whose marrow lesions were malignant marrow-replacing lesions (9 women and 12 men; mean age,  $58 \pm 12.8$  [36-94] years). These subjects were determined to be included in this group because of hot uptake of the lesion in  $^{18}\text{F}$ -fludeoxyglucose positron emission tomographic-computed tomography (CT) ( $n = 9$ ), newly developed radiopharmaceutic uptake on follow-up bone scintigraphy ( $n = 2$ ), a pathologic result from CT-guided biopsy ( $n = 8$ ), and from bone marrow aspiration for patients with a suspected hematologic malignancy ( $n = 2$ ). The malignant marrow-replacing lesions of the subjects were as follows: lung cancer ( $n = 4$ ); pancreatic cancer ( $n = 1$ ); colorectal cancer ( $n = 4$ ); multiple myeloma ( $n = 2$ ); thyroid carcinoma ( $n = 2$ ); nasopharyngeal cancer ( $n = 1$ ); gall bladder adenocarcinoma ( $n = 1$ ); gastric adenocarcinoma ( $n = 1$ ); breast cancer ( $n = 2$ ); prostate cancer ( $n = 2$ ); and hepatocellular carcinoma ( $n = 1$ ).

Group 2 consisted of 11 subjects with benign red marrow depositions (3 women and 8 men; mean age,  $63.6 \pm 16.5$  [38-90] years). These patients were included in this group based on histology (hypercellular red marrow,  $n = 4$ ) and imaging assessment results ( $n = 7$ ). The imaging criteria included no size progression and morphologic change at 2-month and 6-month follow-up MRI (12, 13), no pathologic uptake with bone scan ( $n = 2$ ) or PET/CT ( $n = 5$ ). Other benign lesions were excluded through CT for all patients as follows: no coarse trabeculation to exclude hemangioma, and no sclerosis to rule out lesion

mineralization which can be seen in benign notochordal cell tumor.<sup>14</sup>

## 2. MR Imaging Protocol

MR imaging was performed on a 1.5-T MR imaging scanner (MAGNETOM Avanto, Siemens Healthcare, Erlangen, Germany) with spine matrix coils. In addition to routine sequences including sagittal T1-weighted turbo spin echo (TSE) imaging, fat-suppressed (FS) T1-weighted TSE images in the axial plane and pre- and post-gadolinium (Gd)-enhanced fat-suppressed T1-weighted TSE images (contrast material, 0.1 mmol of gadoterate meglumine [Dotarem; Guerbet, Roissy, France] per kilogram of body weight) in the sagittal plane were included. For T2\*-corrected FF quantification, a three-echo volume interpolated breath-hold gradient-echo sequence (VIBE-Dixon, work-in-progress 432.rev.1, Siemens Healthcare, Erlangen, Germany) was used. It enables to sample one opposed-phase and two in-phase echoes. A T2\* map is estimated from the latter two echoes; the opposed-phase and first in-phase echoes are then corrected for T2\* effects, and are processed by the two-point Dixon water/fat separation algorithm. This sequence automatically reconstructs FF images. The imaging parameters of the pulse sequences used for analysis are summarized in Table 1.

**Table 1.** Summary of Analyzed MR Imaging Parameters

Imaging parameters	Sagittal T1- weighted TSE	Sagittal FS T1- weighted TSE	Sagittal Gd-enhanced FS T1- weighted TSE	Sagittal three-echo VIBE-Dixon
Repetition time (msec)	450	575	575	20
Echo time (msec)	10	10	10	4.76, 7.14, 9.52
Bandwidth (Hz/pixel)	199	199	199	558
Echo train length	3	3	3	1
Flip angle (°)	145	145	145	25
No. of slices	17	17	17	30
Section thickness, gap (mm)	3, 0.3	3, 0.3	3, 0.3	3, 0
Matrix size	410 × 512	410 × 512	410 × 512	192 × 256
Field of view (mm)	500 × 500	500 × 500	500 × 500	400 × 400
Imaging time	4 min, 30 sec	4 min, 50 sec	4 min, 50 sec	1 min, 10 sec

TSE, turbo spin echo; FS, fat suppressed; Gd, gadolinium; VIBE, volume interpolated breath-hold gradient echo.

### 3. Image Analysis

We obtained three parameters for one representative lesion (the largest lesion on the images), if multiple lesions were present, in each subject by using the images. The parameters were the FF, lesion-disc ratio (LDR), and contrast-enhancement ratio (CER). The FF was directly obtained by drawing a region of interest (ROI) of the lesion on the automatically reconstructed FF image obtained from the three-echo VIBE-Dixon sequence. The LDR was obtained from the following equation:  $LDR = (SI \text{ of marrow lesion} / SI \text{ of disc}) \times 100$ , where SI was measured from the images obtained from sagittal T1WI. In a prior report, Zhao et al. described that non-degenerative disc and muscle showed similar accuracy as an internal standard to assess bone marrow pathologies in 1.5-T scanner images, whereas muscle showed superior accuracy compared to non-degenerative disc for the purpose in 3-T scanner images.<sup>15</sup> Thus, in our study, the non-degenerative disc SI was adopted as the internal reference standard to assess marrow lesions, because we used a 1.5-T MR imaging scanner. Additionally, on sagittal images, non-degenerative disc was easier to select than non-fatty muscles. The degeneration of disc was evaluated using Pfirrmann's grading system.<sup>16</sup> The CER was calculated by dividing the difference between the LDR values of post- and pre-Gd-enhanced FS T1WI by the LDR value of pre-Gd-enhanced FS T1WI according to the following equation:  $CER = (LDR_{\text{post Gd-enhanced FS T1WI}} - LDR_{\text{pre Gd-enhanced FS T1WI}}) \times 100 / LDR_{\text{pre Gd-enhanced FS T1WI}}$ , where  $LDR_{\text{post Gd-enhanced FS T1WI}}$  and  $LDR_{\text{pre}}$

Gd-enhanced FS T1WI are the LDR of the lesion on enhanced and unenhanced images, respectively. The SI of a tissue on an MR image is not an absolute value because it is determined by coil loading, the receiver setting at the MR console, and image reconstruction parameters; thus, the SI value must be related to an internal standard.<sup>17</sup> We set the intervertebral disc, which does not generally enhance with Gd, as the internal standard to measure the enhancement degree on pre- and post-Gd-enhanced FS T1WI.

To test whether the disc was enhanced, the signal-to-noise ratio (SNR) of each reference disc was estimated by dividing the SI of the disc by the standard deviation of the background SI. For this calculation, a third-year resident trainee drew the ROIs both for pre- and post-Gd-enhanced FS T1WI at the identical location of the images by copying and pasting the ROIs on an MR imaging work station, as described below. The mean SNRs of the discs were compared between the sequences. And we presumed that the disc was an appropriate internal standard. All three parameters were recorded as percentages.

A round ROI was drawn on an MR imaging workstation by using *syngo* MR software (VB17, Siemens Healthcare, Erlangen, Germany). The ROI for the representative lesion was drawn as large as possible without violating the adjacent marrow. The ROI for the non-degenerative disc (selected on the sagittal T2-weighted image) was drawn at the center of the nucleus pulposus, at the same image slice of the representative lesion; the ROI was drawn as

large as possible without violating the adjacent endplate. For the LDR and CER parameters, the ROI was drawn on the images from T1WI, and the ROI was copied and pasted on the corresponding images taken from pre- and post-Gd-enhanced FS T1WI to obtain the measurement from the identical position for each lesion. However, the ROI for the FF was drawn at the most completely matched images with reference to the T1WI because, given the different matrix and geometry parameters, it was impossible to copy and paste the ROI (Fig 1).

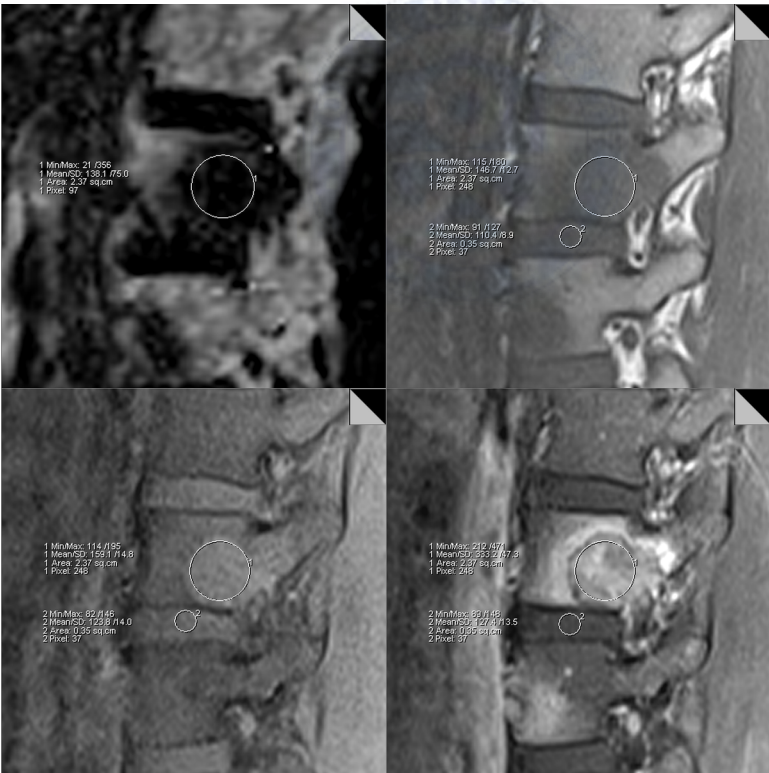


**Fig. 1.** Region of interest (ROI) placement and parameter measurement.

A screen-captured image during ROI placement for parameter measurement of a lesion and a disc on the workstation is shown. The images used for analysis were from a fat-signal fraction (FF) mapping image from the three-point Dixon volume interpolated breath-hold gradient-echo sequence (top left), T1-weighted imaging (T1WI, top right), and pre- (bottom left) and post- (bottom right) gadolinium(Gd)-enhanced fat suppressed (FS) T1WI. The details regarding ROI placement are described in the text. The FF was obtained from the FF mapping sequence image directly by placing the ROI. The lesion-disc ratio (LDR) was obtained from the image of T1WI. The contrast-enhancement ratio (CER) was obtained from images of pre- and post-Gd-enhanced FS T1WI. The calculations for these parameters are described in the text. The images of this capture were obtained from a representative metastatic lesion from gastric cancer in a 57-year-old man. The FF, LDR, and CER were 9.8%, 92.1%, and 157.6% respectively. All parameters indicated that the lesion was malignant.

The average values of three consecutive slices in each target lesion were calculated and recorded. A third-year resident trainee and a radiologist with 11 years of experience in musculoskeletal radiology independently drew the ROIs after the subject order was randomized.

#### 4. Statistical Analysis

The interobserver agreement for measuring parameter values was assessed by using the intraclass correlation coefficient (ICC). The mean values of the parameters were used for further analyses.

By using the paired Student's t test, the mean SNRs of the reference discs were compared between the pre- and post-Gd-enhanced FS T1WI. In order to see if FF, LDR, CER were affected by age and sex as having been reported in a previous report,<sup>18</sup> Spearman correlation coefficient and Mann-Whitney U-test was conducted.

The median values and interquartile range of each group in each parameter were calculated for group 1 and 2 respectively. Since normality assumption was violated when we used the Shapiro-Wilk test ( $p < 0.05$ ), we used nonparametric Mann-Whitney U-test to compare the median values of the three parameters between the two groups.

Receiver operating characteristic (ROC) curves were obtained to evaluate the diagnostic performance of the three parameters and the sensitivities, specificities at the most ideal cut-off values were determined by the ROC curve. Confidence intervals for the area under the curve (AUC), sensitivity, and specificity were computed to account for sampling variation in the data.

False-positive (erroneously defined as malignancy) and false-negative (erroneously defined as benign) results were counted for each parameter and were analyzed by two investigators in consensus regarding explanatory

factors. For false-negative results, the pathology of the lesion was recorded. The usefulness of low signal intensity of the marrow lesions on T1-weighted imaging as a tool for the differentiation between malignant and benign marrow lesions has well been validated in prior studies,<sup>19,20</sup> and we aimed to assess whether the FF quantification can be an additional tool for the differentiation by comparing it with CER. To compare the diagnostic performance of FF and CER, their areas under the curves were compared by using the DeLong test. The sensitivities and specificities of the two parameters were also compared by using McNemar's test.

All statistical analyses were performed by using SAS software (V 9.2, SAS Institute, Carey, NC, USA). P-values < 0.05 were considered statistically significant.

### III. RESULTS

All overall interobserver agreements between the two readers for measuring parameter values indicated perfect agreement. The ICC values for FF, LDR, and CER were 0.991, 0.997, and 0.965, respectively. The mean ROI size of the readers was  $90.0 \pm 58.6$  (17.2–236.5) mm<sup>2</sup> for lesions and  $22.1 \pm 19.7$  (5.7–53.2) mm<sup>2</sup> for discs.

The Spearman correlation coefficient for the three parameters and age were all below 0.3 with non-significant P-value (> 0.05) indicating no correlation between age and the parameters. Also the result of the Mann-Whitney U-test

showed that the median values of the three parameters were not significantly different in male and female. These results advocate that age and sex would not affect our analysis.

In the reference disc SNR enhancement assessment, the mean disc SNR of pre-Gd-enhanced FS T1WI was  $44.6 \pm 15.4$  (15.5–72.0) and that of post-Gd-enhanced FS T1WI was  $43.4 \pm 16.0$  (15.1–72.2). No difference in the SNR was observed between pre- and post-Gd-enhanced FS T1WI ( $p = 0.168$ ), indicating that the means discs were not enhanced and could be used as an internal standard.

The median values of each parameter in each group are summarized in Table 2. All three parameters showed a median difference between group 1 and 2 with statistical significance (Table 2). The AUC of each parameter, the optimal cut-off values obtained from the ROC curve, and the resultant sensitivity and specificity of each parameter are summarized in Table 3.

**Table 2.** Comparison of Median Values for the Parameters between Malignant-replacing Lesion and Benign Red Marrow

Deposition Groups

Parameter	Median (IQR)	<i>P</i> -value*
FF		<0.001
Group 1	12.8 (10.6–16.3)	
Group 2	37.3 (26.0–48.0)	
LDR		0.004
Group 1	91 (83.1–103.3)	
Group 2	120 (101.0–133.9)	
CER		0.038
Group 1	99.4 (87.9–110.2)	
Group 2	64 (55.6–93.7)	

*P*-value\* : statistical significance in the difference of median values between group 1 and group 2 for each parameter.

IQR, interquartile range; Group 1, malignant marrow-replacing lesion; Group 2, benign red marrow deposition; FF, fat-signal fraction; LDR, lesion-disc ratio; CER, contrast-enhancement ratio.

**Table 3.** Diagnostic Performance of Each Parameter Determined Through Receiver Operating Characteristic Curve Analysis

Parameter	AUC	Cutoff values (%) <sup>*</sup>	Sensitivity (%)	Specificity (%)	<i>P</i> -value <sup>†</sup>
FF	0.961 (0.826–0.998)	≤ 16.8%	85.7 (18/21; 63.7–97.0)	100 (11/11; 71.5–100)	<0.001
LDR	0.805 (0.627–0.923)	≤ 114.8%	100 (21/21; 83.9–100)	63.6 (7/11; 30.8–89.1)	0.002
CER	0.727 (0.542–0.869)	> 93.7%	66.7 (14/21; 43.0–85.4)	81.8 (9/11; 48.2–97.7)	0.038

The numbers in parentheses in the AUC column are 95% confidence intervals.

The numbers in parenthesis in the sensitivity and specificity columns are the counts used for the calculation and 95% confidence intervals.

Cutoff values (%)<sup>\*</sup>: The lesions were considered malignant when the FF was 16.8% or less, the LDR was 114.8% or less, and the CER was 93.7% or greater.

*P*-value<sup>†</sup>: *p*-value of AUC.

AUC, area under the receiver operating characteristic curve; FF, fat-signal fraction; LDR, lesion-disc ratio; CER, contrast-enhancement ratio.

In the analyses of false-positive and false-negative results, FF showed three false-negative results (metastases from prostate [n = 1], colon [n = 1], and breast cancer [n = 1]) (Fig 2). LDR showed four false-positive results (one from pathologically proven hypercellular red marrow; three clinically categorized as red marrow deposition) (Fig 3). CER showed two false-positive (both categorized as red marrow deposition clinically) (Fig 4) and seven false-negative results (metastases from rectal [n = 2], thyroid [n = 1], nasopharyngeal [n = 1], lung [n = 1], and prostate cancer [n = 1] and plasma cell myeloma [n=1 ]) (Fig 5).

In the comparison of AUCs between FF and CER, the AUC of FF was significantly higher compared to that of CER ( $p = 0.030$ ). In the McNemar's test for the comparison of sensitivity and specificity between FF and CER, the difference of the sensitivity ( $p = 0.157$ ), specificity ( $p = 0.157$ ) were not significant.

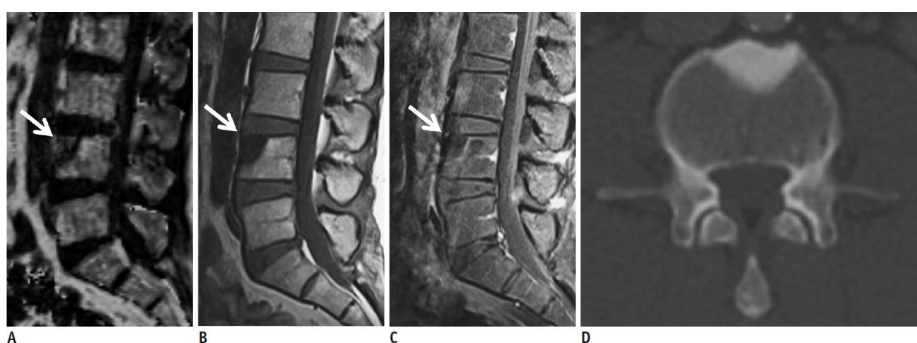


**Fig 2.** An example of a false-negative result (erroneously defined as benign) of FF illustrated from MR images and a computed tomography (CT) image

obtained from a 54-year-old man.

He was referred for assessment of a metastatic bone lesion of the 4<sup>th</sup> lumbar (L4) vertebra from prostate cancer, which was suspected on bone scintigraphy by newly developed radiopharmaceutical uptake.

Images obtained from MR imaging (FF mapping sequence [A], T1WI [B], post-Gd-enhanced FS T1WI [C]), and a non-contrast CT image (D) of the L4 vertebral body are shown. The FF image revealed high FF of the lesion (arrow in A), which indicated a considerable amount of fat. The lesion showed low signal intensity on T1WI (arrow in B), and did not show avid enhancement (arrow in C). Because the lesion newly developed during follow-up and appeared to be a space-occupying lesion rather than a degenerative change or osteitis related to enthesitis, it was categorized as group 1 (malignant marrow-replacing lesion) and was considered a metastatic bone lesion from prostate cancer. The FF, LDR, and CER were calculated as 28.1%, 36.7%, and 49.5% respectively, which shows that FF and CER erroneously indicated the lesion was benign (false-negative results), whereas LDR correctly indicated the lesion was malignant (true-positive result). The axial non-contrast CT image (D) revealed the osteoblastic characteristics of this metastatic lesion.

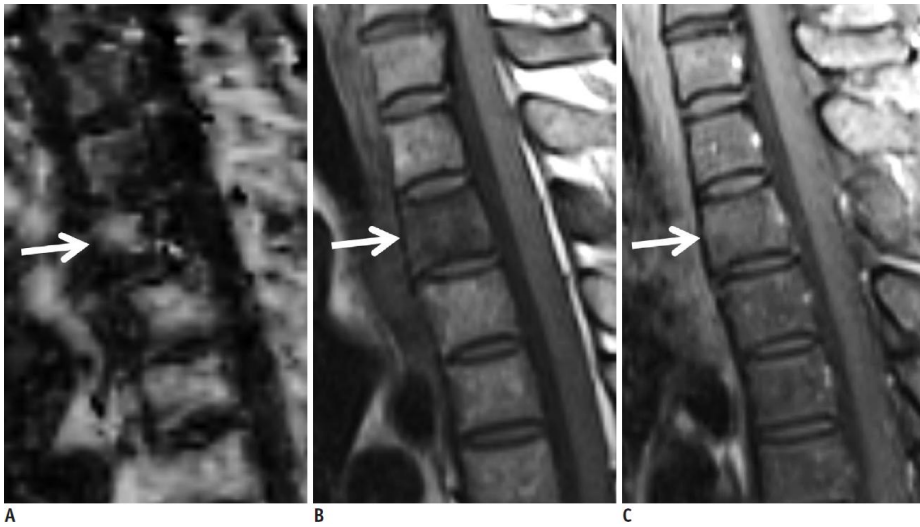


**Fig 3.** An example of a false-positive result (erroneously defined as malignant) of LDR illustrated from MR images obtained from a 46-year-old woman.

She was referred for assessment of the cause of back pain, and was incidentally found to have a marrow lesion of the 2<sup>nd</sup> thoracic (T2) vertebra.

Images obtained from the FF mapping sequence (A), T1WI (B), and post-Gd-enhanced FS T1WI (C) are shown. The FF image revealed high FF of the lesion (arrow in A), which indicated a considerable amount of fat. The lesion showed low signal intensity on T1WI (arrow in B), and did not show avid enhancement (arrow in C). The lesion almost completely replaced the T2 vertebral body, and the ROI was drawn as described in the text. CT-guide biopsy revealed that the lesion was hypercellular red marrow (80% cellularity) without evidence of malignancy; hence, the lesion was categorized as group 2 (benign red marrow deposition). The FF, LDR, and CER were calculated as

39.8%, 88.9%, and 81.5%, respectively, which shows that FF and CER correctly indicated the lesion was benign (true-negative result), whereas LDR erroneously indicated the lesion was malignant (false-positive result).

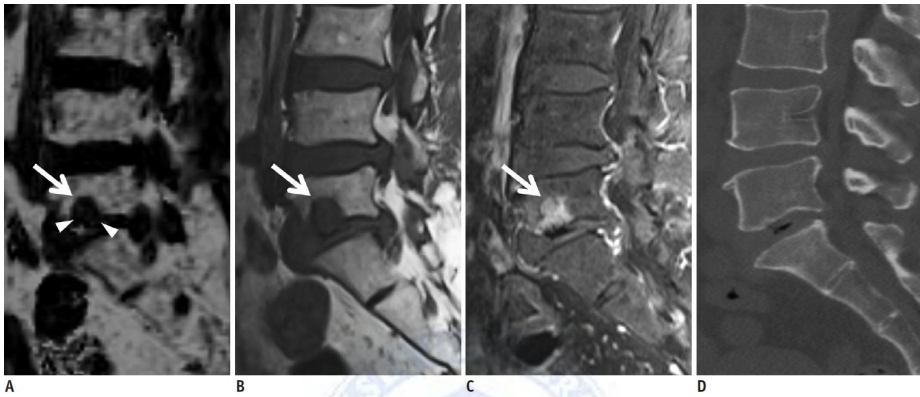


**Fig 4.** An example of a false-positive result (erroneously defined as malignant) of CER illustrated from MR images obtained from a 66-year-old woman.

She was referred for assessment of the cause of back pain, and was incidentally found to have a marrow lesion of the 5<sup>th</sup> lumbar (L5) vertebra.

Images obtained from the FF mapping sequence (A), T1WI (B), and post-Gd-enhanced FS T1WI (C) of the L5 vertebral body are shown. The FF image showed a focal lesion (arrow in A). Multifocal high FF of the lesion (arrowheads in A) was observed, which indicated multifocal fat deposition. The lesion showed low signal intensity on T1WI (arrow in B), and relatively avid enhancement (arrow in C). Because the lesion did not show a morphologic or signal change on the 6-month follow-up MR imaging and did

not show mineralization or an osteolytic lesion at the corresponding area on CT scan (D), the lesion was categorized as group 2 (benign red marrow deposition). The FF, LDR, and CER were calculated as 26.0%, 101.8%, and 132.4% respectively, which shows that LDR and CER erroneously indicated the lesion was malignant (false-positive result), whereas FF correctly indicated the lesion was benign (true-negative result).

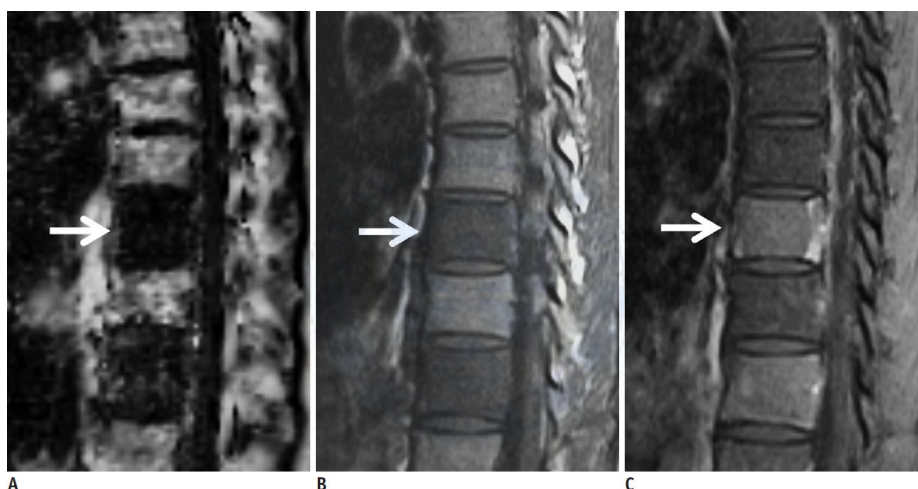


**Fig. 5.** An example of a false-negative result (erroneously defined as benign) of CER illustrated from MR images obtained from a 42-year-old man.

He was referred for assessment of metastasis at the vertebral column, which was suspected on 18F-fludeoxyglucose (FDG) positron-emission tomographic (PET)-computed tomography (CT).

Images obtained from the FF mapping sequence (A), T1WI (B), and post-Gd-enhanced FS T1WI (C) of the T9 vertebral body. The FF image revealed low FF of the lesion (arrow in A), which indicated a low amount of

fat. The lesion showed low signal intensity on T1WI (arrow in B), and did not show avid enhancement (arrow in C). Because the 18F-FDG PET-CT of this patient showed multiple increased FDG uptakes of the skeleton and lung, the T9 vertebral lesion was categorized as group 1 (malignant marrow-replacing lesion). The lesion almost completely replaced the vertebral body, and the ROI was drawn as described in the text. The FF, LDR, and CER were calculated as 12.8%, 82.5%, and 51.6% respectively, which shows that CER erroneously indicated the lesion was benign (false-negative result), whereas FF and LDR correctly indicated the lesion was malignant (true-positive result).

#### IV. DISCUSSION

We assessed whether FF obtained from vertebral body lesions is feasible in differentiating malignant marrow-replacing lesions from benign red marrow deposition. We focused on red marrow deposition as the benign lesion. Although we used the chemical-shift imaging method utilized in the previous studies,<sup>4-7,9,21</sup> we attempted to measure the FF itself unlike these previous studies as we thought this approach is more reasonable as stated above. Regarding the use of marrow fat to differentiate between malignant versus benign bone marrow lesions, previous investigators focused on “signal drop” on opposed-phase imaging because they postulated the coexistence of fat and

water in marrow,<sup>4-7,9,21</sup> which is possible when bone marrow is not completely replaced by space-occupying lesions, would cause signal drop in opposed-phase imaging. These investigators measured the signal drop of opposed-phase imaging and suggested variable cut-off values to differentiate between various benign and malignant vertebral lesions (Table 4). With these parameters, the sensitivity and specificity of differentiating between benign and malignant lesion were 88.8–95% and 80.4–100%, respectively.<sup>4-7,9,21</sup> The sensitivity (85.7%) and specificity (100%) of FF in our study were comparable to those of previous studies that utilized chemical-shift imaging, which means our study did not show improvement in diagnostic performance of chemical-shift imaging as compared with previous studies. However, we believe our results unveiled the feasibility of FF as a tool for differentiation between benign and malignant focal bone marrow lesions, and further investigation with a larger study population appears to be needed.

**Table 4.** Summary of Previous Studies Related to Chemical-shift Imaging for Differentiation between Benign and Malignant Lesions

Study	Total number of patients (lesions)*	Lesions that were differentiated <sup>†</sup>	Parameter	Suggested cut-off value	Sensitivity	Specificity
Disler DG. <sup>(9)</sup>	30 patients (31)	Non-neoplastic lesion (14) Neoplastic lesion (17)	SI ratio ( $SI_{\text{opposed-phase}}/SI_{\text{in-phase}}$ )	> 0.81	95%	95%
Zampa V. <sup>(7)</sup>	86 patients (86)	Benign lesion (41) Malignant lesion (45)	SI ratio ( $SI_{\text{opposed-phase}}/SI_{T1W1}$ )	>1.2	88.8%	80.4%
Eito K. <sup>(21)</sup>	108 patients (190)	Normal vertebrae (90) Compression fracture (100) Non-neoplastic (73) Neoplastic (27)	SI ratio ( $SI_{\text{opposed-phase}}/SI_{\text{in-phase}}$ )	None <sup>§</sup>	N/A	N/A
Zajick DC. <sup>(4)</sup>	75 patients (569) 92 patients (215)	Normal vertebrae (569) Benign lesion (164) Malignant lesion (51)	% decrease of $SI_{\text{opposed-phase}}$ compared with $SI_{\text{in-phase}}$	≤20%	N/A	N/A
Erly WK. <sup>(6)</sup>	21 patients (49)	Benign compression fracture (29) Malignant lesion (20)	SI ratio ( $SI_{\text{opposed-phase}}/SI_{\text{in-phase}}$ )	>0.8	95%	89%
Ragab Y. <sup>(5)</sup>	40 patients (40)	Compression fracture (40) Osteoporotic (20) Neoplastic (20)	% decrease of $SI_{\text{opposed-phase}}$ compared with $SI_{\text{in-phase}}$	≤35%	95%	100%

\*: the numbers in parentheses in this column are the counts of lesions.

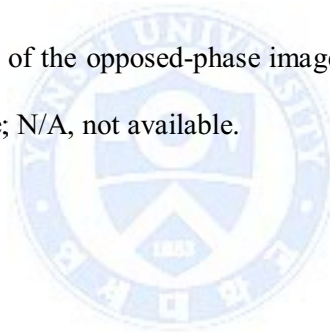
Lesions that were differentiated<sup>†</sup>: normal, benign, and malignant lesions that were described and assessed. The numbers in parentheses of this column are the counts of lesions.

Suggested cut-off value<sup>‡</sup>: lesions were defined as malignant when the suggested cut-off value was satisfied for each parameter.

None<sup>§</sup>: Eito et al. calculated the mean value of each lesion group, but did not estimate the cut-off value for differentiating between the groups.

SI, signal intensity; SI<sub>opposed-phase</sub>, signal intensity of the opposed-phase image; SI<sub>in-phase</sub>, signal intensity of the in-phase image;

SI<sub>T1WI</sub>, signal intensity of the T1-weighted image; N/A, not available.



A high FF erroneously indicated that three lesions were benign: two sclerotic metastases from prostate or breast cancer and one from metastatic colon cancer. Zajick et al. reported that some metastatic lesions show large signal drop on opposed-phase imaging, mimicking benign bone lesions.<sup>4</sup> They attributed the variability of metastatic lesions from lytic to sclerotic states, with sclerotic lesions having lower SIs.<sup>4</sup> Although Zajick et al. did not completely explain the reason for this observation, we believe the two sclerotic lesions showing false-negative results in our study are consistent with it. We adopted three-echo Dixon integrated into the VIBE sequence. The Dixon technique is a well-established imaging sequence for discrimination between water and fat protons on the basis of their resonant frequency difference.<sup>22</sup> Three-echo Dixon technique has been developed to correct T2\* decay due to intra-voxel static field inhomogeneity that depends on tissue structure and chemical properties. Three-echo Dixon have been proven to provide a highly reproducible and accurate results in fat quantification as compared with two-echo Dixon without T2\* correction.<sup>23</sup>

Even with correction of T2\* effects, FF quantification may be confounded by other effects like the multi-spectral nature of fat.<sup>24</sup> As a result, the three-echo VIBE-DIXON sequence may produce errors similar to those observed in previous studies that utilized other chemical-shift imaging techniques, and this topic should be investigated further. However, we have no plausible explanation for the false-negative result for colon cancer

metastasis in our study.

Hypothetically, the FF values for malignant-replacing lesions should be near 0% because the lesion replaces bone marrow. However, the FF cut-off value for differentiation between malignant-replacing lesions and benign red marrow deposition was unexpectedly high in our study (16.8%). Although many previous studies assessed the liver rather than bone marrow, it is known that the T1 and T2\* effects should be minimized to measure FF accurately, because all MR signals are subject to T1 and T2/T2\* relaxation.<sup>11</sup> We believe the T2\* effect was minimized in our study, because we adopted a sequence that corrects the effect of T2\* decay by using signals at three different echo times which was validated in a prior report.<sup>10</sup> However, the 25° flip angle used in our study might have produced the T1 effect, which is known to cause FF overestimation. Cassidy et al. recommended a flip angle of 5–10° and a repetition time of  $\leq 100$  msec to minimize the T1 effect for liver fat quantification<sup>11</sup>; the sequence parameters that minimize the T1 effect for bone marrow might be different from these parameters, but we could not find any related references. Hence, we optimized our sequence empirically, and we could not minimize the flip angle to  $< 25^\circ$  to assure appropriate image quality with respect to the SNR ratio at the commencement of our study. We believe 25° was not adequate for minimizing the T1 effect, given the unexpectedly high FF of our study. Further validation of FF quantification sequences is needed. T1 effect reduction could be achieved by using a low flip angle and a

more accurate correction of the confounding T2\* effect and multi-spectral fat nature by using signals from more echo time points.

The sensitivity and specificity of T1WI in previous studies performed with 1.5-T scanners were 62.5–100% and 92–93.8% for differentiating benign and malignant lesions, respectively.<sup>15,20</sup> Although the sensitivity of our study was comparable to that of these studies, the specificity was far lower due to different analysis methods<sup>20</sup> and the selection of benign subjects for comparison.<sup>15</sup> Nevertheless, LDR is a sensitive method in daily practice for detection or screening of marrow signal abnormality and we do not believe that our study supports that FF can replace LDR in that regard. Rather, we expect that the FF would play a complementary role for additional differentiation with its high specificity, which would be superior to CER, since CER showed poorer performance compared to FF in our study. Gd-enhanced MR imaging needed to be compared with the FF measurement in the performance of differentiation between benign and malignant marrow lesions as previous studies have already elucidated its usefulness in this aspect.<sup>13,25,26</sup>

Our study had several limitations. First, the small number of study subjects might have biased our results. Second, the pulse sequence for FF quantification was not validated through a bone marrow phantom, because this is technically difficult. However, we have elucidated that a T2\*-corrected FF map using the three-echo VIBE-Dixon sequence is at least feasible for

differentiating between malignant marrow-replacing lesions and benign red marrow deposition of vertebrae. Third, not all assessed lesions were pathologically proven, because it would be unethical to biopsy lesions with a high probability of malignancy or benignancy in a clinical setting. Fourth, we adopted only LDR for the parameters on T1WI, although qualitative assessment of imaging findings (e.g., bull's eye sign)<sup>27</sup> is useful for differentiating between malignant and benign bone lesions. This may also explain why the specificity of T1WI was lower than expected in our study. However, this qualitative assessment was beyond the scope of our study.

In conclusion, T2\*-corrected FF measurement using a three-echo VIBE-Dixon sequence is feasible and is expected to play a complementary role for distinguishing benign red marrow deposition from malignant bone marrow-replacing lesions of vertebrae.

## **V. CONCLUSION**

Fat-signal fraction measurement using T2\*-corrected three-echo VIBE DIXON sequence is feasible and shows more accurate diagnostic performance than CER in distinguishing benign red marrow deposition from malignant bone marrow-replacing lesions.

## REFERENCES

1. Swartz PG, Roberts CC. Radiological reasoning: bone marrow changes on MRI. *AJR Am J Roentgenol* 2009;193:S1-4, Quiz S5-9.
2. Shah LM, Hanrahan CJ. MRI of spinal bone marrow: part I, techniques and normal age-related appearances. *AJR Am J Roentgenol* 2011;197:1298-308.
3. Tall MA, Thompson AK, Vertinsky T, Palka PS. MR imaging of the spinal bone marrow. *Magn Reson Imaging Clin N Am* 2007;15:175-98,
4. Zajick DC, Jr., Morrison WB, Schweitzer ME, Parellada JA, Carrino JA. Benign and malignant processes: normal values and differentiation with chemical shift MR imaging in vertebral marrow. *Radiology* 2005;237:590-6.
5. Ragab Y, Emad Y, Gheita T, Mansour M, Abou-Zeid A, Ferrari S, et al. Differentiation of osteoporotic and neoplastic vertebral fractures by chemical shift {in-phase and out-of phase} MR imaging. *Eur J Radiol* 2009;72:125-33.
6. Erly WK, Oh ES, Outwater EK. The utility of in-phase/opposed-phase imaging in differentiating malignancy from acute benign compression fractures of the spine. *AJNR Am J Neuroradiol* 2006;27:1183-8.
7. Zampa V, Cosottini M, Michelassi C, Ortori S, Bruschini L, Bartolozzi C. Value of opposed-phase gradient-echo technique in distinguishing between benign and malignant vertebral lesions. *Eur Radiol*

- 2002;12:1811-8.
8. Wismer GL, Rosen BR, Buxton R, Stark DD, Brady TJ. Chemical shift imaging of bone marrow: preliminary experience. *AJR Am J Roentgenol* 1985;145:1031-7.
  9. Disler DG, McCauley TR, Ratner LM, Kesack CD, Cooper JA. In-phase and out-of-phase MR imaging of bone marrow: prediction of neoplasia based on the detection of coexistent fat and water. *AJR Am J Roentgenol* 1997;169:1439-47.
  10. Kuhn JP, Evert M, Friedrich N, Kannengiesser S, Mayerle J, Thiel R, et al. Noninvasive quantification of hepatic fat content using three-echo dixon magnetic resonance imaging with correction for T2\* relaxation effects. *Invest Radiol* 2011;46:783-9.
  11. Cassidy FH, Yokoo T, Aganovic L, Hanna RF, Bydder M, Middleton MS, et al. Fatty liver disease: MR imaging techniques for the detection and quantification of liver steatosis. *Radiographics* 2009;29:231-60.
  12. Geith T, Schmidt G, Biffar A, Dietrich O, Durr HR, Reiser M, et al. Comparison of qualitative and quantitative evaluation of diffusion-weighted MRI and chemical-shift imaging in the differentiation of benign and malignant vertebral body fractures. *AJR Am J Roentgenol* 2012;199:1083-92.
  13. Chen WT, Shih TT, Chen RC, Lo HY, Chou CT, Lee JM, et al. Blood perfusion of vertebral lesions evaluated with gadolinium-enhanced

- dynamic MRI: in comparison with compression fracture and metastasis. *J Magn Reson Imaging* 2002;15:308-14.
14. Yamaguchi T, Iwata J, Sugihara S, McCarthy EF, Jr., Karita M, Murakami H, et al. Distinguishing benign notochordal cell tumors from vertebral chordoma. *Skeletal Radiol* 2008;37:291-9.
  15. Zhao J, Krug R, Xu D, Lu Y, Link TM. MRI of the spine: image quality and normal-neoplastic bone marrow contrast at 3 T versus 1.5 T. *AJR Am J Roentgenol* 2009;192:873-80.
  16. Pfirrmann CW, Metzdorf A, Zanetti M, Hodler J, Boos N. Magnetic resonance classification of lumbar intervertebral disc degeneration. *Spine (Phila Pa 1976)* 2001;26:1873-8.
  17. Buckley DL, Parker GJM. Measuring contrast agent concentration in T1-weighted dynamic contrast-enhanced MRI. In: Jackson A, Buckley DL, Parker GJM. *Dynamic contrast-enhanced magnetic resonance imaging in oncology*. 1st ed. Berlin; London: Springer, 2004;69-79.
  18. Griffith JF, Yeung DK, Ma HT, Leung JC, Kwok TC, Leung PC. Bone marrow fat content in the elderly: a reversal of sex difference seen in younger subjects. *J Magn Reson Imaging* 2012;36:225-30.
  19. Vande Berg BC, Malghem J, Lecouvet FE, Maldague B. Classification and detection of bone marrow lesions with magnetic resonance imaging. *Skeletal Radiol* 1998;27:529-45.
  20. Carroll KW, Feller JF, Tirman PF. Useful internal standards for

- distinguishing infiltrative marrow pathology from hematopoietic marrow at MRI. *J Magn Reson Imaging* 1997;7:394-8.
21. Eito K, Waka S, Naoko N, Makoto A, Atsuko H. Vertebral neoplastic compression fractures: assessment by dual-phase chemical shift imaging. *J Magn Reson Imaging* 2004;20:1020-4.
  22. Dixon WT. Simple proton spectroscopic imaging. *Radiology* 1984;153:189-94.
  23. Kovanlikaya A, Guclu C, Desai C, Becerra R, Gilsanz V. Fat quantification using three-point dixon technique: in vitro validation. *Acad Radiol* 2005;12:636-9.
  24. Reeder SB, Bice EK, Yu H, Hernando D, Pineda AR. On the performance of T2\* correction methods for quantification of hepatic fat content. *Magn Reson Med* 2012;67:389-404.
  25. Rahmouni A, Divine M, Mathieu D, Golli M, Dao TH, Jazaerli N, et al. Detection of multiple myeloma involving the spine: efficacy of fat-suppression and contrast-enhanced MR imaging. *AJR Am J Roentgenol* 1993;160:1049-52.
  26. Breault SR, Heye T, Bashir MR, Dale BM, Merkle EM, Reiner CS, et al. Quantitative dynamic contrast-enhanced MRI of pelvic and lumbar bone marrow: effect of age and marrow fat content on pharmacokinetic parameter values. *AJR Am J Roentgenol* 2013;200:W297-303.
  27. Schweitzer ME, Levine C, Mitchell DG, Gannon FH, Gomella LG.

Bull's-eyes and halos: useful MR discriminators of osseous metastases.

Radiology 1993;188:249-52.



ABSTRACT(IN KOREAN)

Three-echo VIBE Dixon 자기공명영상을 이용한 척추의 골수를 대체하는 악성 병변과 양성 적색골수 침착의 감별

<지도교수 김 성 준>

연세대학교 대학원 의학과

김 용 표

**서론:** 척추 자기공명 VIBE (three-echo volume interpolated breath-hold gradient echo ) Dixon 영상에서 얻은 T2\*-corrected fat-signal fraction map을 통하여 척추의 골수를 대체하는 악성 병변과 양성 적색골수를 감별하고자 하였다.

**대상 및 방법:** 척추의 골수 이상소건을 평가하기 위해 척추 자기공명영상을 촬영하였던 32명의 환자에서 32개의 병변을 평가하였고, 병변은 21개의 악성 골수 병변과 11개의 양성 적색골수 침착으로 그룹을 나누었다. 1.5-T MR imaging scanner 에서 3가지 sequence를 통한 다음과 같은 3가지 영상지표를 산출하였다 : 1) three-echo VIBE Dixon 영상을 통한 지방분율 (fat fraction, FF), 2) T1강조 영상을 통한 병변-디스크 비율 (lesion-disc ratio, LDR), 3) pre- and post-gadolinium enhanced fat-suppressed T1강조 영상을 통한 조영증강 비율 (contrast-enhancement ratio, CER).

각 병변에서 3가지 영상지표를 구하기 위하여 T1 강조영상 시상면, T1 fat suppressed 시상면, 조영증강 T1 fat suppressed 시상면, VIBE Dixon fat fraction 시상면에서 region of interest (ROI)를 측정하였다. Receiver operating curve(ROC) 분석을 통하여 영상지표 사이의 진단능을 비교하고 cut off value를 사정하고, FF와 CER 영상지표 사이의 민감도(sensitivity), 특이도(specificity), 정확도(accuracy)를 McNemar 검증을 통하여 비교하였다.

**결과:** FF, LDR, CER의 Area under the curves (AUCs)는 각각 0.96, 0.80, 0.72 이었다. 민감도 ( $p = 0.157$ )와 특이도 ( $p = 0.157$ )의 차이는 유의하지 않았지만, FF와 CER 사이의 진단능 비교에 있어서 FF는 CER에 비해 유의하게 큰 AUC를 보였다.

**결론:** T2\*-corrected three-echo VIBE Dixon 자기공명영상을 통한 FF (지방분율) 측정은 척추의 골수를 대체하는 악성 병변과 양성 적색골수 침착의 감별에 있어서 CER (조영증강비율)보다 정확한 진단능을 보였다.

---

핵심되는 말 : 자기공명영상, 척추, 지방분율, 골수

## PUBLICATION LIST

Kim YP, Kannengiesser S, Paek MY, Kim S, et al. Differentiation between focal malignant marrow-replacing lesions and benign red marrow deposition of the spine with T2\*-corrected fat-signal fraction map using a three-echo volume interpolated breath-hold gradient echo Dixon sequence. Korean J Radiol 2014;15:781-91.

